




Labdane conjugates protect cardiomyocytes from doxorubicin-induced cardiotoxicity

Irene Cuadrado¹ | Sandra Oramas-Royo² | Laura González-Cofrade¹ |
 Ángel Amesty² | Sonsoles Hortelano³  | Ana Estévez-Braun²  |
 Beatriz de las Heras¹ 

¹Departamento de Farmacología, Farmacognosia y Botánica, Facultad de Farmacia, Universidad Complutense de Madrid (UCM), Madrid, Spain

²Departamento de Química Orgánica, Instituto Universitario de Bio-Organica Antonio González, Universidad de La Laguna, La Laguna, Tenerife, Spain

³Unidad de Terapias Farmacológicas, Área de Genética Humana, Instituto de Investigación de Enfermedades Raras (IIER), Instituto de Salud Carlos III, Madrid, Spain

Correspondence

Beatriz de las Heras, Sonsoles Hortelano and Ana Estévez-Braun, Departamento de Farmacología, Farmacognosia y Botánica, Facultad de Farmacia, Universidad Complutense de Madrid (UCM), Plaza Ramón y Cajal s/n-28040, Madrid, Spain.

Email: lsheras@ucm.es, shortelano@isciii.es and aestebra@ull.edu.es

Funding information

European Regional Development Fund; Ministerio de Ciencia, Innovación y Universidades (MICIU), Grant/Award Number: RTI2018-094356-BC21; Instituto de Salud Carlos III, Grant/Award Numbers: PI17/00012, PI20/00018

Abstract

The cardiovascular side effects associated with doxorubicin (DOX), a wide spectrum anticancer drug, have limited its clinical application. Therefore, to explore novel strategies with cardioprotective effects, a series of new labdane conjugates were prepared (**6a–6c** and **8a–8d**) from the natural diterpene labdanodiol (**1**). These hybrid compounds contain anti-inflammatory privileged structures such as naphthalimide, naphthoquinone, and furanonaphthoquinone. Biological activity of these conjugates against DOX-induced cardiotoxicity was tested in vitro and the potential molecular mechanisms of protective effects were explored in H9c2 cardiomyocytes. Three compounds **6c**, **8a**, and **8b** significantly improved cardiomyocyte survival, via inhibition of reactive oxygen species-mediated mitogen-activated protein kinase signaling pathways (extracellular signal-regulated kinase and c-Jun N-terminal kinase) and autophagy mediated by Akt activation. Some structure–activity relationships were outlined, and the best activity was achieved with the labdane–furanonaphthoquinone conjugate **8a** having an *N*-cyclohexyl substituent. The findings of this study pave the way for further investigations to obtain more compounds with potential cardioprotective activity.

KEYWORDS

cardioprotection, doxorubicin, labdane diterpenes, naphthalimide, naphthoquinone

1 | INTRODUCTION

Doxorubicin (DOX) is an effective and widely prescribed cytotoxic agent commonly used to treat various human hematological and solid cancers. However, the severe cardiovascular side effects leading to

cardiomyopathy and congestive heart failure have limited its clinical use in chemotherapy (Al-Malky et al., 2020). Cardiomyocytes have been considered as the main target for DOX. Multiple molecules and signaling pathways have been implicated in the pathogenesis of DOX-induced cardiotoxicity, including oxidative stress, cardiac inflammation,

This is an open access article under the terms of the Creative Commons Attribution-NonCommercial-NoDerivs License, which permits use and distribution in any medium, provided the original work is properly cited, the use is non-commercial and no modifications or adaptations are made.

© 2022 The Authors. *Drug Development Research* published by Wiley Periodicals LLC.

cardiomyocyte apoptosis, and autophagy dysregulation (Prathumsap et al., 2020; Yu et al., 2018). Several stress-responsive signaling pathways, such as the mitogen-activated protein kinases (MAPKs), c-Jun N-terminal kinase (JNK), and extracellular signal-regulated kinase (ERK), regulate inflammation, apoptosis, and autophagy, contributing to DOX-induced cell death. This drug also mediates damage at various steps of cardiac energy metabolism, affecting the sensitivity of cardiac cells to apoptosis and leading to defects in the AMP-activated protein kinase (AMPK) signaling pathway (Octavia et al., 2012).

Natural products, in particular diterpenes, are a valuable chemical group in drug discovery due to their wide spectrum of biological activities, including anti-inflammatory (Cuadrado et al., 2012; de las Heras & Hortelano, 2009; González-Cofrade et al., 2020; Song et al., 2022; Tran et al., 2017), antioxidant (P. Gong et al., 2022), and anticancer (Abdullah et al., 2021; Islam, 2017; Través et al., 2013) activities.

In the search for new therapeutic strategies for cardioprotection, diterpenes and their derivatives constitute a good starting point since a number of diterpenes have shown protective activities. Among them, kirenol showed cardioprotection through its antiapoptotic and prosurvival effects (Alzahrani et al., 2021). Moreover, other kaurane and labdane diterpenes also exhibited cardioprotective effects against ischemic myocardial injury (Cuadrado-Berrocal et al., 2015; Gao et al., 2021; Marco, 2020). The basic skeletal structure of labdane diterpenes presents two parts: a fused decalin system (C-1–C-10) and a branched six-carbon side chain (C-11–C-16) at C-9. The remaining four carbons (C-17–C-20) are methyl groups attached at C-8, C-4, and C-10 of the decalin system, respectively. In the present work, from the natural labdane diol (1) (Amaro-Luis & Adrian, 1982) and through its side chain, a novel series of labdane hybrid compounds containing naphthalimide or naphthoquinone were prepared using as linker a triazole or a furan ring (6a–6c and 8a–8d). Moreover, the protective effects of these compounds were evaluated in a DOX-induced cardiotoxicity model. Results showed that three derivatives 6c, 8a, and 8b, exhibited cardioprotective effects by increasing cell viability in a dose–response manner through regulation of oxidative stress and autophagy. Conjugate 8a was identified as an applicable agent to prevent DOX-induced cardiotoxicity.

2 | MATERIALS AND METHODS

2.1 | General experimental procedures

Nuclear magnetic resonance (NMR) spectra were recorded in CDCl₃ at 400, 500, or 600 MHz for ¹H NMR and 100, 125, or 150 MHz for ¹³C NMR. Chemical shifts (δ) are given in parts per million, and coupling constants (*J*) in hertz (Hz). ¹H and ¹³C spectra were referenced using the solvent signal as an internal standard. High-resolution electron ionization mass spectrometry (HREIMS) was recorded using a high-resolution magnetic trisector mass analyzer. Analytical thin-layer chromatography plates used were Polygram-Sil G/UV254. Preparative thin-layer chromatography was carried out with Analtech silica gel GF

plates (20 × 20 cm², 1000 μm) using appropriate mixtures of ethyl acetate and hexanes. All solvents and reagents were purified by standard techniques reported (Perrin & Amarego, 1988) or used as supplied from commercial sources. The labdane diol (1) used as starting material was obtained from *Oxylobus glanduliferus* (Asteraceae) following the procedure described in (Amaro-Luis & Adrian, 1982). Characterization of labdane diol (1) and synthetic procedures and characterization data for synthesized compounds 2–4, 7, and 9–10 are included in the Supporting information.

2.1.1 | General procedure for the synthesis of labdane conjugates 6a–6c

A solution of the labdane azide (4) (1 equiv) and the corresponding alkyne (2 equiv) in 3 ml of CH₂Cl₂ (dichloromethane [DCM]) was added to a mixture of CuSO₄·5H₂O (4 mol%) and sodium ascorbate (12 mol%) in 3 ml of water. The reaction mixture was stirred vigorously at room temperature until the disappearance of the alkyne. Then, it was extracted with DCM (3 × 15 ml), the organic phases were collected, dried over anhydrous MgSO₄, filtered, and the solvent was eliminated under reduced pressure. The residue was purified by preparative thin-layer chromatography (TLC) with hexanes:EtOAc (7:3) as eluent.

2.1.2 | Preparation of labdane–naphthoquinone conjugate 6a

Following the experimental procedure, from 81.7 mg (0.26 mmol) of azide 4 and 108.8 mg (0.51 mmol) of *O*-propargyl-1,4-naphthoquinone, compound 6a was obtained as an orange solid (10.8 mg, 8%); ¹H-NMR (500 MHz, CDCl₃) δ 8.12 (1H, d, *J* = 7.5 Hz), 8.09 (1H, d, *J* = 7.5 Hz), 7.76 (1H, t, *J* = 7.5 Hz), 7.71 (2H, m), 6.43 (1H, s), 5.26 (2H, s), 4.40 (2H, m), 1.94 (4H, m), 1.76 (2H, m), 1.59 (1H, m), 1.53 (3H, s), 1.46 (2H, m), 1.40 (2H, m), 1.26 (2H, m), 1.13 (3H, m), 1.00 (3H, d, *J* = 6.6 Hz), 0.96 (2H, m), 0.92 (3H, s), 0.88 (3H, s), 0.82 (3H, s); ¹³C-NMR (125 MHz, CDCl₃) δ 184.8 (C), 180.1 (C), 159.1 (C), 141.7 (C), 140.7 (C), 134.5 (CH), 133.5 (CH), 133.2 (C), 131.3 (C), 126.8 (CH), 126.4 (CH), 125.8 (C), 123.3 (CH), 111.4 (CH), 63.3 (CH₂), 52.1 (CH), 49.0 (CH₂), 42.0 (CH₂), 39.1 (C), 37.4 (CH₂), 37.3 (CH₂), 37.2 (CH₂), 33.8 (CH₂), 33.5 (CH₃), 33.4 (C), 31.6 (CH), 25.4 (CH₂), 21.8 (CH₃), 20.3 (CH₃), 20.0 (CH₃), 19.3 (CH₃), 19.2 (2 CH₂); EIMS *m/z* 529 [M⁺, 20], 515 (18), 340 (19), 191 (54), 121 (32), 109 (44), 91 (38), 55 (100); HREIMS 529.3329 (calcd for C₃₃H₄₃N₃O₃ [M⁺] 529.3304).

2.1.3 | Preparation of labdane–naphthoquinone conjugate 6b

Following the experimental procedure, from 76.4 mg (0.24 mmol) of azide 4 and 101.3 mg (0.48 mmol) of *N*-propargyl-1,4-naphthoquinone, compound 6b was obtained as an orange solid

(20.7 mg, 16%); $^1\text{H-NMR}$ (500 MHz, CDCl_3) δ 8.10 (1H, d, $J = 7.7$ Hz), 8.06 (1H, d, $J = 7.7$ Hz), 7.74 (1H, t, $J = 7.5$ Hz), 7.63 (1H, t, $J = 7.5$ Hz), 7.52 (1H, s), 6.35 (1H, s), 5.83 (1H, s), 4.51 (2H, d, $J = 5.5$ Hz), 4.38 (2H, m), 1.93 (4H, m), 1.75 (2H, m), 1.58 (1H, m), 1.52 (3H, s), 1.42 (5H, m), 1.25 (2H, m), 1.12 (3H, m), 0.99 (3H, d, $J = 6.5$ Hz), 0.96 (1H, m), 0.92 (3H, s), 0.87 (3H, s), 0.82 (3H, s); $^{13}\text{C-NMR}$ (125 MHz, CDCl_3) δ 183.2 (C), 181.7 (C), 147.7 (C), 142.8 (C), 140.7 (C), 134.9 (CH), 133.6 (C), 132.3 (CH), 130.7 (C), 126.5 (CH), 126.4 (CH), 125.9 (C), 121.7 (CH), 101.9 (CH), 52.1 (CH), 49.0 (CH_2), 42.0 (CH_2), 39.2 (C), 38.5 (CH_2), 37.4 (CH_2), 37.4 (CH_2), 37.3 (CH_2), 33.8 (CH_2), 33.5 (CH_3), 33.4 (C), 31.7 (CH), 25.5 (CH_2), 21.8 (CH_3), 20.3 (CH_3), 19.7 (CH_3), 19.3 (CH_3), 19.2 (2 CH_2); EIMS m/z 528 [M^+ , 47], 340 (100), 191 (27), 174 (51), 121 (23), 110 (48), 105 (46), 81 (34), 55 (56); HREIMS 528.3472 (calcd for $\text{C}_{33}\text{H}_{44}\text{N}_4\text{O}_2$ [M^+] 528.3464).

2.1.4 | Preparation of labdane-naphthalimide conjugate **6c**

Following the experimental procedure, from 100.0 mg (0.31 mmol) of azide **4** and 147.8 mg (0.63 mmol) of *N*-propargyl-1,8-naphthalimide, compound **6c** was synthesized as an orange solid (34.1 mg, 20%); $^1\text{H-NMR}$ (500 MHz, CDCl_3) δ 8.63 (2H, d, $J = 7.3$ Hz), 8.22 (2H, d, $J = 8.2$ Hz), 7.76 (2H, t, $J = 7.5$ Hz), 7.63 (1H, s), 5.52 (2H, s), 4.31 (2H, m), 1.90 (4H, m), 1.70 (2H, m), 1.56 (1H, m), 1.49 (3H, s), 1.39 (5H, m), 1.23 (2H, m), 1.09 (3H, m), 0.95 (3H, d, $J = 6.3$ Hz), 0.93 (1H, m), 0.90 (3H, s), 0.87 (3H, s), 0.81 (3H, s); $^{13}\text{C-NMR}$ (125 MHz, CDCl_3) δ 164.1 (2 C), 143.8 (C), 140.8 (C), 134.2 (2 CH), 131.8 (C), 131.6 (2 CH), 128.5 (C), 127.1 (2 CH), 125.7 (C), 123.1 (2 C), 122.8 (CH), 52.1 (CH), 48.7 (CH_2), 42.0 (CH_2), 39.1 (C), 37.5 (CH_2), 37.4 (CH_2), 37.3 (CH_2), 35.5 (CH_2), 33.8 (CH_2), 33.5 (CH_3), 33.4 (C), 31.7 (CH), 25.5 (CH_2), 21.8 (CH_3), 20.3 (CH_3), 19.7 (CH_3), 19.3 (CH_3), 19.2 (CH_2), 19.2 (CH_2); EIMS m/z 552 [M^+ , 60], 347 (100), 235 (46), 198 (46), 180 (81), 152 (36), 81 (39), 55 (62); HREIMS 552.3470 (calcd for $\text{C}_{35}\text{H}_{44}\text{N}_4\text{O}_2$ [M^+] 552.3464).

2.1.5 | General procedure for the synthesis of labdane-furonaphthoquinone conjugates **8a–8d**

A solution of 2-hydroxy-1,4-naphthoquinone, 1.2 equiv of aldehyde **7**, and 0.1 equiv of ethylenediamine diacetate (EDDA) in 7 ml of toluene was treated with 1.2 equiv of the corresponding isocyanide. The reaction mixture was heated under reflux until the disappearance of the starting material. Then, it was cooled to room temperature and the toluene was removed under reduced pressure. The residue was purified by preparative -TLC using hexanes:EtOAc (7:3).

2.1.6 | Preparation of labdane-furonaphthoquinone conjugate **8a**

Following the general procedure, from 37.9 mg (0.13 mmol) of aldehyde **7**, 16.2 μl (0.13 mmol) of cyclohexyl isocyanide and

18.9 mg (0.11 mmol) of lawsone, compound **8a** was obtained as a blue solid (37.9 mg, 50%); $^1\text{H-NMR}$ (600 MHz, CDCl_3) δ 8.15 (1H, dd, $J = 1.3, 7.7$ Hz), 8.05 (1H, dd, $J = 1.3, 7.7$ Hz), 7.67 (1H, td, $J = 1.3, 7.6$ Hz), 7.59 (1H, td, $J = 1.3, 7.6$ Hz), 4.26 (1H, d, $J = 8.9$ Hz), 3.83 (1H, m), 2.59 (1H, dd, $J = 6.2, 14.2$ Hz), 2.40 (1H, dd, $J = 8.2, 14.2$ Hz), 2.06 (3H, m), 1.98 (3H, m), 1.91 (1H, dd, $J = 6.4, 17.3$ Hz), 1.77 (3H, m), 1.66 (3H, m), 1.56 (1H, m), 1.49 (3H, s), 1.42 (5H, m), 1.25 (4H, m), 1.14 (1H, m), 1.11 (1H, t, $J = 4.6$ Hz), 1.08 (1H, dd, $J = 1.8, 12.6$ Hz), 0.94 (3H, d, $J = 6.4$ Hz), 0.93 (3H, s), 0.87 (3H, s), 0.82 (3H, s); $^{13}\text{C-NMR}$ (150 MHz, CDCl_3) δ 183.2 (C), 168.5 (C), 160.2 (C), 142.9 (C), 141.0 (C), 134.0 (C), 133.8 (CH), 133.1 (C), 133.0 (C), 132.0 (CH), 126.3 (CH), 126.2 (CH), 125.6 (C), 98.8 (C), 52.5 (CH), 52.1 (CH), 42.0 (CH_2), 39.1 (C), 38.1 (CH_2), 37.3 (CH_2), 35.2 (CH), 34.3 (CH_2), 34.2 (C), 33.8 (CH_2), 33.5 (CH_3), 30.2 (CH_2), 25.9 (CH_2), 25.6 (CH_2), 25.5 (CH_2), 24.9 (CH_2), 24.8 (CH_2), 21.8 (CH_3), 20.3 (CH_3), 19.7 (CH_3), 19.6 (CH_3), 19.2 (2 CH_2); EIMS m/z 555 [M^+ , 52], 308 (39), 226 (88), 191 (32), 83 (33), 55 (100); HREIMS 555.3713 (calcd for $\text{C}_{37}\text{H}_{49}\text{NO}_3$ [M^+] 555.3712).

2.1.7 | Preparation of labdane-furonaphthoquinone conjugate **8b**

Following the general procedure, from 35.1 mg (0.12 mmol) of aldehyde **7**, 16.7 μl (0.12 mmol) of 2-morpholinoethyl isocyanide and 17.4 mg (0.10 mmol) of lawsone, compound **8b** was obtained as a blue solid (60.3 mg, 85%); $^1\text{H-NMR}$ (600 MHz, CDCl_3) δ 8.14 (1H, d, $J = 7.5$ Hz), 8.05 (1H, d, $J = 7.5$ Hz), 7.67 (1H, t, $J = 7.4$ Hz), 7.61 (1H, t, $J = 7.4$ Hz), 3.74 (4H, m), 3.60 (2H, m), 2.67 (2H, m), 2.54 (4H, m), 2.44 (1H, m), 2.01 (3H, m), 1.92 (1H, m), 1.77 (3H, m), 1.62 (2H, m), 1.53 (3H, s), 1.45 (1H, m), 1.39 (1H, m), 1.29 (3H, m), 1.11 (3H, m), 0.95 (3H, d, $J = 6.4$ Hz), 0.94 (3H, s), 0.87 (3H, s), 0.82 (3H, s); $^{13}\text{C-NMR}$ (150 MHz, CDCl_3) δ 183.2 (C), 168.6 (C), 161.3 (C), 160.7 (C), 142.9 (C), 140.9 (C), 133.9 (C), 133.8 (CH), 133.2 (C), 132.1 (CH), 126.4 (CH), 126.2 (CH), 125.6 (C), 98.7 (C), 67.2 (2 CH_2), 56.7 (CH_2), 53.2 (2 CH_2), 52.0 (CH), 41.9 (CH_2), 39.1 (CH_2), 39.1 (C), 38.1 (CH_2), 37.2 (CH_2), 35.2 (CH), 34.3 (C), 33.8 (CH_2), 33.5 (CH_3), 30.1 (CH_2), 25.9 (CH_2), 21.8 (CH_3), 20.3 (CH_3), 19.7 (2 CH_3), 19.2 (2 CH_2); EIMS m/z 586 [M^+ , 11], 191 (5), 114 (6), 100 (100), 69 (11); HREIMS 586.3766 (calcd for $\text{C}_{37}\text{H}_{50}\text{N}_2\text{O}_4$ [M^+] 586.3771).

2.1.8 | Preparation of labdane-furonaphthoquinone conjugate **8c**

Following the general procedure, from 28.7 mg (0.10 mmol) of aldehyde **7**, 12.1 μl (0.10 mmol) of benzyl isocyanide and 14.4 mg (0.08 mmol) of lawsone, compound **8c** was synthesized as a blue solid (39.1 mg, 72%); $^1\text{H-NMR}$ (600 MHz, CDCl_3) δ 8.15 (1H, dd, $J = 0.8, 7.5$ Hz), 8.06 (1H, dd, $J = 0.8, 7.5$ Hz), 7.68 (1H, td, $J = 1.1, 7.5$ Hz), 7.61 (1H, t, $J = 1.1, 7.5$ Hz), 7.36 (4H, m), 7.32 (1H, m), 4.68 (3H, m), 2.62 (1H, dd, $J = 6.1, 14.3$ Hz), 2.38 (1H, dd, $J = 8.5, 14.3$ Hz), 1.97 (2H, m), 1.92 (1H, dd, $J = 6.1, 17.5$ Hz), 1.76 (2H, d, $J = 12.5$ Hz), 1.62 (2H, m),

1.59 (3H, s), 1.55 (1H, m), 1.41 (3H, m), 1.25 (2H, m), 1.09 (3H, m), 0.92 (3H, m), 0.91 (3H, d, $J = 6.4$ Hz), 0.87 (3H, s), 0.82 (3H, s); ^{13}C -NMR (150 MHz, CDCl_3) δ 183.1 (C), 169.1 (C), 160.0 (C), 143.2 (C), 140.9 (C), 138.0 (C), 133.8 (CH), 133.7 (C), 133.2 (C), 133.0 (C), 132.2 (CH), 129.1 (2 CH), 128.2 (CH), 127.9 (2 CH), 126.4 (CH), 126.3 (CH), 125.6 (C), 98.8 (C), 52.0 (CH), 47.38 (CH_2), 41.9 (CH_2), 39.1 (C), 39.1 (CH_2), 37.9 (CH_2), 37.2 (CH_2), 35.1 (CH), 33.7 (CH_2), 33.6 (C), 33.5 (CH_3), 30.2 (CH_2), 25.8 (CH_2), 21.8 (CH_3), 20.2 (CH_3), 19.7 (CH_3), 19.5 (CH_3), 19.2 (2 CH_2); EIMS m/z 563 [M^+ , 26], 318 (19), 191 (23), 91 (100), 55 (8); HREIMS 563.3385 (calcd for $\text{C}_{38}\text{H}_{45}\text{NO}_3$ [M^+] 563.3399).

2.1.9 | Preparation of compound 8d

Following the general procedure, from 24.0 mg (0.08 mmol) of aldehyde 7, 9.0 μl (0.08 mmol) of *tert*-butyl isocyanide and 12.0 mg (0.07 mmol) of lawsone, compound 8d was obtained as a blue solid (7.8 mg, 21%). ^1H -NMR (500 MHz, CDCl_3) δ 8.15 (1H, dd, $J = 1.0$, 7.6 Hz), 8.05 (1H, dd, $J = 1.0$, 7.6 Hz), 7.67 (1H, td, $J = 1.3$, 7.5 Hz), 7.60 (1H, t, $J = 1.3$, 7.5 Hz), 4.24 (1H, s), 2.62 (1H, dd, $J = 6.0$, 14.0 Hz), 2.35 (1H, dd, $J = 8.3$, 14.0 Hz), 2.00 (3H, m), 1.91 (1H, dd, $J = 6.3$, 17.8 Hz), 1.77 (2H, m), 1.60 (5H, m), 1.51 (3H, s), 1.48 (9H, s), 1.39 (2H, m), 1.27 (1H, m), 1.13 (1H, m), 1.08 (1H, dd, $J = 1.7$, 12.6 Hz), 0.94 (3H, s), 0.93 (3H, d, $J = 6.3$ Hz), 0.87 (3H, s), 0.82 (3H, s); ^{13}C -NMR (150 MHz, CDCl_3) δ 182.3 (C), 169.0 (C), 160.3 (C), 143.5 (C), 141.1 (C), 133.9 (C), 133.7 (CH), 133.3 (C), 133.0 (C), 132.1 (CH), 126.3 (CH), 126.2 (CH), 121.6 (C), 100.9 (C), 54.0 (C), 52.1 (CH), 42.0 (CH_2), 39.1 (C), 38.1 (CH_2), 37.3 (CH_2), 36.5 (C), 35.2 (CH), 33.8 (CH_2), 33.5 (CH_3), 30.5 (CH_2), 30.3 (3 CH_3), 25.9 (CH_2), 21.9 (CH_3), 20.3 (CH_3), 19.7 (CH_3), 19.7 (CH_3), 19.3 (CH_2), 19.2 (CH_2); EIMS m/z 529 [M^+ , 20], 514 (14), 357 (10), 340 (18), 174 (26), 83 (24), 55 (100); HREIMS 529.3566 (calcd for $\text{C}_{35}\text{H}_{47}\text{NO}_3$ [M^+] 529.3566).

2.2 | Biological assays

2.2.1 | Cell culture

H9c2 embryonic rat heart-derived cells and MCF-7 breast cancer cells were obtained from the American Type Culture Collection (ATCC). The cells were cultured in Dulbecco's modified Eagle's medium (Sigma), containing 10% fetal bovine serum, 100 U/ml penicillin, and 100 $\mu\text{g}/\text{ml}$ streptomycin, at 37°C in a humidified incubator containing 5% CO_2 .

2.2.2 | Cell viability

To evaluate the cytotoxicity of DOX and tested compounds, cell viability assays were performed using the 3-(4,5-dimethylthiazol-2-yl)-2,5-diphenyl-2H-tetrazolium bromide (MTT) and lactate dehydrogenase (LDH) methods. Briefly, H9c2 and MCF7 cells were

seeded at a density of 5×10^4 cells/well and 1×10^4 cells/well, respectively, in 96-well plates for 24 h. Then, cells were treated with DOX (Sigma) in the absence or presence of compounds. MTT (Sigma; 5 mg/ml for H9c2 or 2 mg/ml for MCF7) reagent was added to the medium for 1 h at 37°C. Then, the formazan was dissolved in dimethyl sulfoxide (100 μl). Absorbance was measured at 540 nm with a microplate reader (BMG Labtech). LDH was determined in cell supernatants by measuring the conversion of pyruvate to lactate, and analyzed spectrophotometrically at 490 nm, using CytoTox96[®] kit (Promega).

2.2.3 | Cardioprotective activity

The cardioprotective effects of compounds were tested in a DOX-induced H9c2 cardiomyocytes model. H9c2 cells were treated with compounds at 20 μM and exposed to 1 μM of DOX for 24 h to cause impairment and decreases in cell viability. After that, cell viability assays were performed to determine the potential protection of the compounds.

Measurement of reactive oxygen species (ROS): Intracellular ROS levels in H9c2 cells were evaluated by monitoring the oxidation of 2',7'-dichlorofluorescein-diacetate (DCFH-DA) (Sigma) to fluorescent dichlorofluorescein. Cells were treated with DOX (1 μM) in the absence or presence of compounds or *N*-acetyl-cysteine (NAC) as ROS inhibitor (1 mM) (Sigma). Then, cells were incubated with 10 μM DCFH-DA at 37°C in the dark for 30 min. ROS level was fluorimetrically evaluated at 485/550 nm for 24 h.

Western blot: Cell lysates were extracted as previously reported (Cuadrado et al., 2011) and later subjected to sodium dodecyl sulfate-polyacrylamide gel electrophoresis (SDS-PAGE) electrophoresis. The gels were transferred onto a Hybond-PVDF membrane and, after blocking, were incubated with anti-pAkt, anti-Akt, anti-pAMPK, anti-AMPK, p62 (Santa Cruz), anti-pERK1/2, anti-ERK1/2, anti-pJNK, and anti-JNK (Cell Signaling). Glycer-aldehyde 3-phosphate dehydrogenase (Abcam) and β -actin (Sigma) were used as a loading control. After further incubation with horseradish peroxidase-conjugated secondary antibodies for 2 h, the specific protein bands were developed by the ECL detection system (Amersham).

2.2.4 | Statistical analysis

All values have been expressed as mean \pm SD. The statistical significance was tested using Sigmaplot 11.0 software (Systat Software). Data were analyzed by one-way analysis of variance. A p value < 0.05 was recognized as a significant difference. The estimated half-maximal inhibitory concentration (IC_{50}) value of the cytotoxic effect of DOX was calculated using GraphPad Prism 8.0 (GraphPad Software) (nonlinear regression).

3 | RESULTS AND DISCUSSION

3.1 | Chemistry

We decided to study the effect of an extension of the structure of the labdane skeleton through its side chain by incorporating other privileged structures with anti-inflammatory activity such as naphthalimides (H. H. Gong et al., 2016; Kamal et al., 2013), naphthoquinones (Liang et al., 2013; Luo et al., 2010; Moon et al., 2007; Tanaka et al., 1986; Tseng et al., 2013; Wang et al., 2014; Yang et al., 2014), and furanonaphthoquinones (Soares et al., 2017).

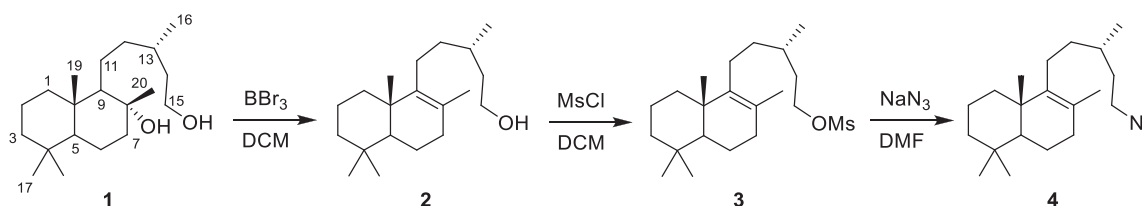
The introduction of these privileged structures was carried out following two different approaches, namely, a copper(I)-catalyzed Huisgen 1,3-dipolar cycloaddition reaction (Rostovtsev et al., 2002) and an isonitrile-based multicomponent reaction (MCR) (Jiménez-Alonso et al., 2011).

Regarding the first approach, it implies the preparation of a labdanoyl azide intermediate (4) as is shown in Scheme 1. Thus, the treatment of labdanediol (1) with BBr_3 in DCM for 24 h afforded

compound 2 in 83% yield. The terminal hydroxyl group was converted quantitatively into the corresponding mesyl derivative (3) by treatment with methanesulfonyl chloride in DCM, and finally, the labdanoyl azide 4 was obtained when 3 was reacted with sodium azide in dimethylformamide.

Next, the reaction of labdanoyl azide (4) with *O*-propargyl-1,4-naphthoquinone, *N*-propargyl-1,4-naphthoquinone, and *N*-propargyl-1,8-naphthalimide, in the presence of $\text{CuSO}_4 \cdot 5\text{H}_2\text{O}$ /sodium ascorbate, afforded the corresponding conjugates with the triazole ring as a linker between the labdane and the 1,4-naphthoquinone (6a–6b) and 1,8-naphthalimide (6c) moieties (Table 1). Compounds 6a–6c were obtained in low-to-moderate yields.

The preparation of labdane–furanonaphthoquinone conjugates was achieved via a MCR from 2-hydroxy-1,4-naphthoquinone, the corresponding isonitrile, and the labdanoyl aldehyde (7). This last compound was quantitatively obtained by the oxidation of compound 2 with pyridinium chlorochromate/DCM. Scheme 2 shows a plausible formation of the labdane–furanonaphthoquinone conjugates. First, a Knoevenagel condensation of lawsone (2-hydroxy-1,4-naphthoquinone) and aldehyde



SCHEME 1 Preparation of labdanoyl azide (4). DCM, dichloromethane; DMF, dimethylformamide.

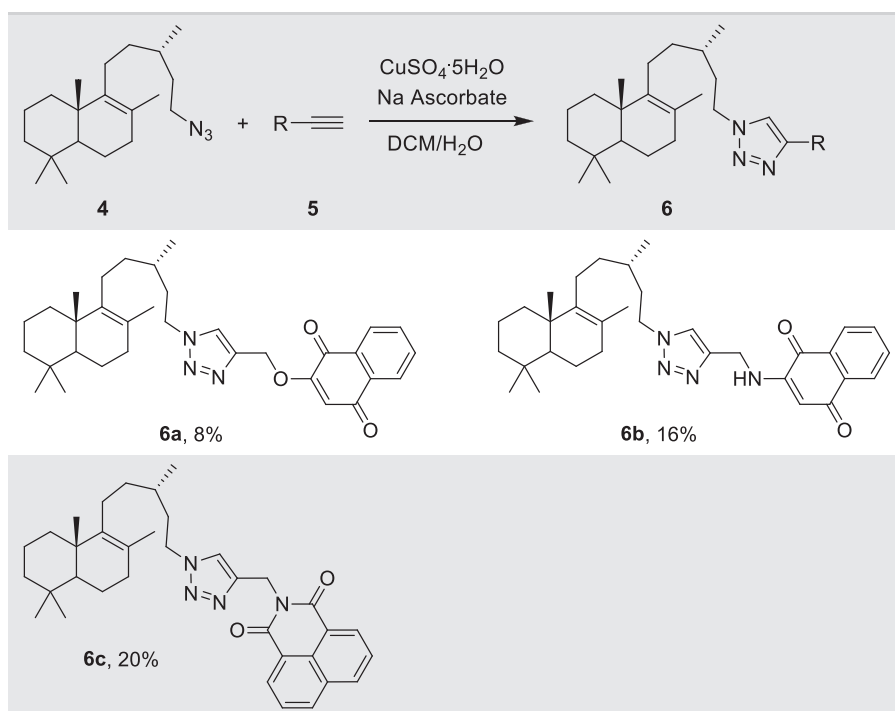
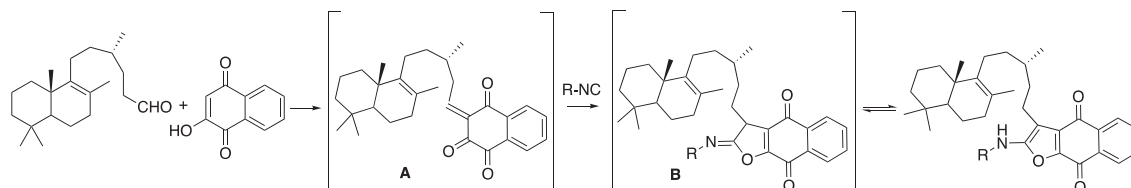


TABLE 1 Synthesis and structure of 1,2,3-triazole-labdane derivatives (6a–6c)

Abbreviation: DCM, dichloromethane.

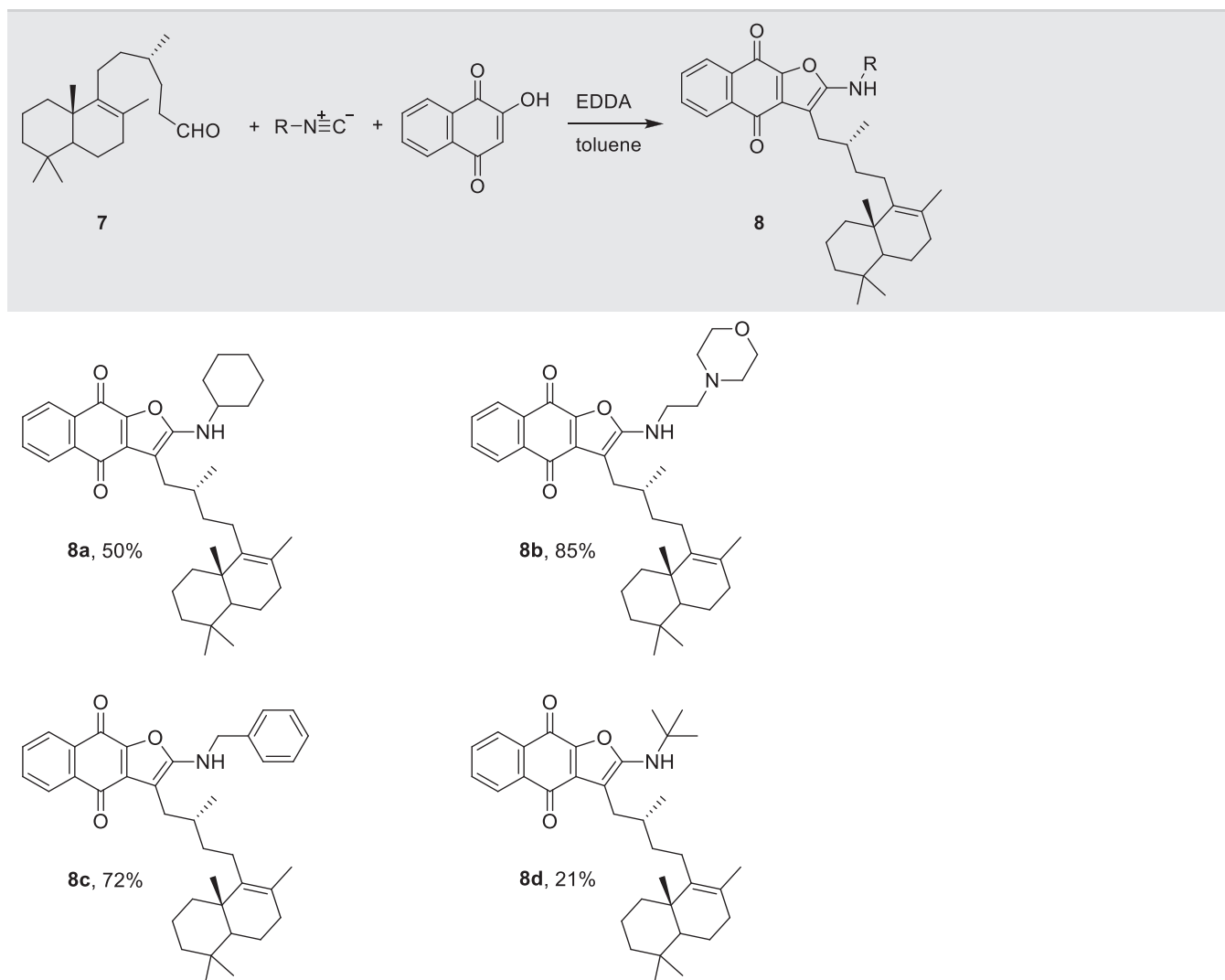
7 takes place to yield a reactive intermediate quinone methide **A**. **B** is an iminolactone intermediate. Next, a [4 + 1] cycloaddition reaction between the isocyanide and the electron-deficient enone (**A**) affords an iminolactone intermediate (**B**). The posterior isomerization of iminolactone (**B**) leads to the formation of the corresponding furan conjugate.

In Table 2 appears the structures and yields obtained when the reaction was carried out using different isocyanides. The best yields were achieved with 2-morpholinoethyl (**8b**) and benzyl (**8c**) isocyanides.



SCHEME 2 Plausible formation of labdane-furanonaphthoquinone conjugates. A: reactive intermediate quinone methide; B: iminolactone intermediate.

TABLE 2 Structure and yields of conjugates **8a–8d** via MCR



Abbreviations: EDDA, ethylenediamine diacetate; MCR, multicomponent reaction.

cytotoxicity of the starting diterpenes **1**, **2** and the labdane conjugates (**6a–6c**, **8a–8d**) was evaluated. The tested compounds did not show any cytotoxicity at a concentration level of 20 μM , with the exception of compound **1** (Figure 1b).

The potential of labdane derivatives as cardioprotective agents was evaluated in cells treated with DOX in the presence of the nontoxic compounds. DOX (1 μM) significantly reduced cell viability by $47.71 \pm 1.40\%$. Among them, three labdane conjugates **6c**, **8a**, and

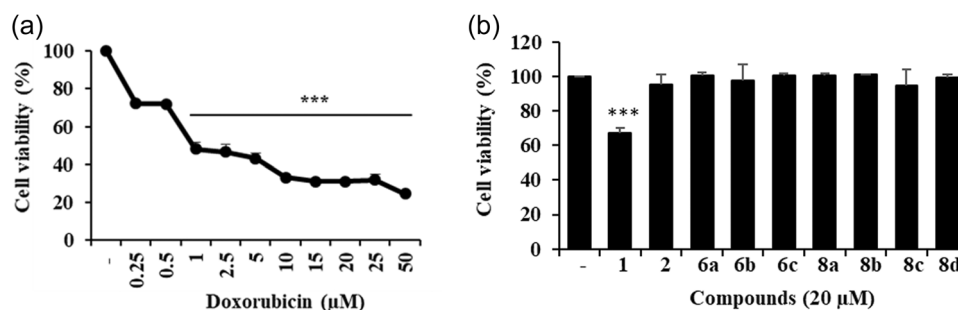


FIGURE 1 Cell viability after treatment with DOX and diterpene derivatives (**1**, **2**, **6a–6c**, and **8a–8d**). (a) H9c2 was treated with DOX (0.25–50 μM) for 24 h or (b) with derivatives (20 μM) for 24 h. Cell viability was determined by MTT assay and results are reported as mean \pm SD ($n = 3$). *** $p < .001$ versus untreated cells. DOX, doxorubicin; MTT, 3-(4,5-dimethylthiazol-2-yl)-2,5-diphenyl-2H-tetrazolium bromide.

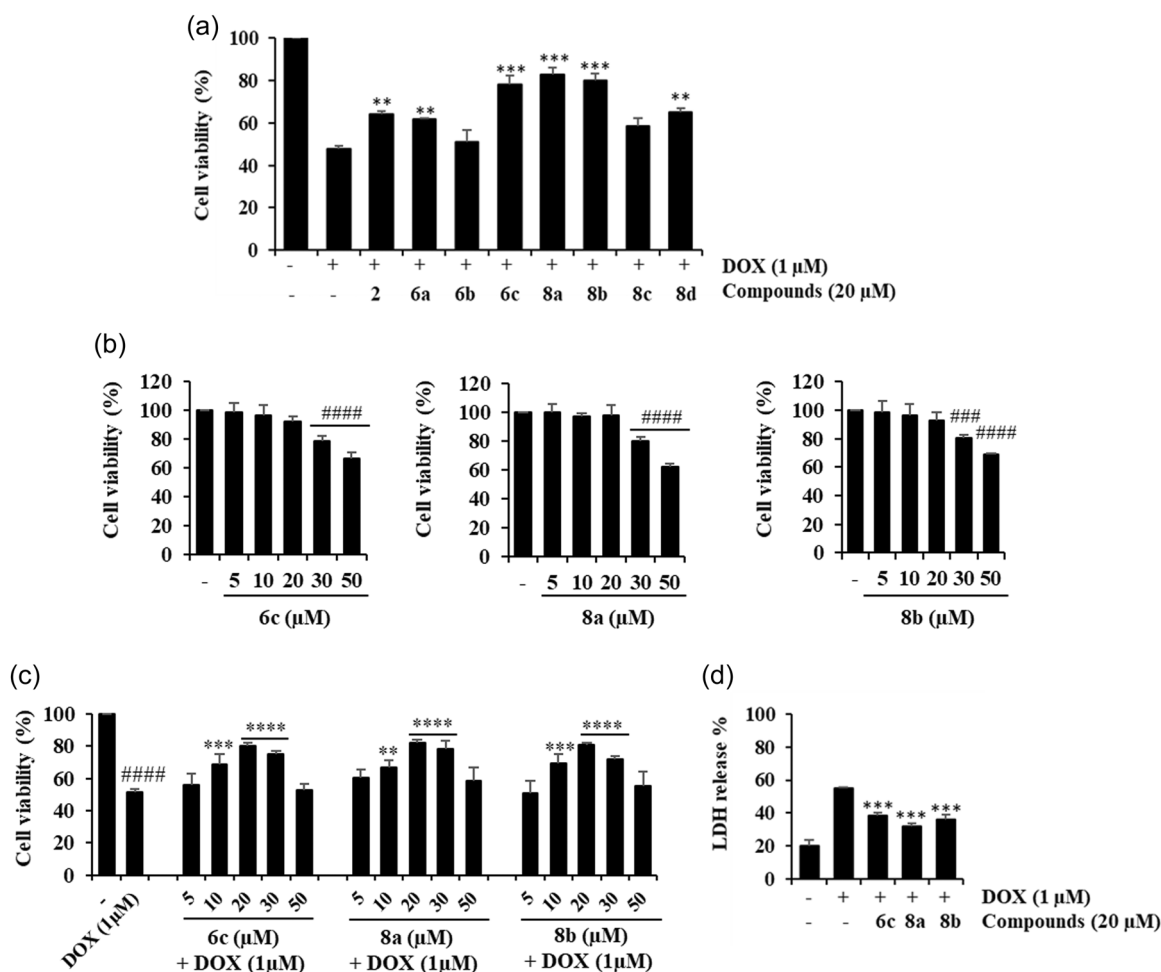


FIGURE 2 Diterpene conjugates **6c**, **8a**, and **8b** attenuated DOX-induced cardiotoxicity in H9c2 rat cardiomyocytes. (a) Cell viability was measured by MTT after incubation for 24 h with DOX (1 μM) or cotreatment with nontoxic compounds (20 μM). (b) Cell viability after treatment with **6c**, **8a**, and **8b** (5–50 μM) for 24 h, determined by MTT assay. (c) Effects of conjugates (5–50 μM) cotreated with DOX (1 μM) for 24 h on cell viability carried out by MTT assay. (d) LDH release after exposure to DOX or combined treatment with **6c**, **8a**, and **8b** at 20 μM . Results are reported as the mean of cell viability \pm SD ($n = 3$). ### $p < .001$ and #### $p < .0001$ versus untreated cells; * $p < .01$, ** $p < .001$, and **** $p < .0001$ versus DOX-treated cells. DOX, doxorubicin; LDH, lactate dehydrogenase; MTT, 3-(4,5-dimethylthiazol-2-yl)-2,5-diphenyl-2H-tetrazolium bromide.

8b showed high cardioprotective potential, which was manifested by a significant increase in the percentage of the viable cells in the presence of DOX ($78.06 \pm 4.42\%$, $82.72 \pm 3.11\%$, and $80.20 \pm 2.87\%$, respectively) (Figure 2a). Cytotoxicity of active conjugates **6c**, **8a**, and **8b** was tested in the range 5–50 μM , with IC_{50} values of 73.5, 60.7, and 80.6 μM , respectively (Figure 2b). Treatment with labdane conjugates attenuated DOX-induced injury in a dose-dependent manner up to 20 μM (Figure 2c). This concentration was selected for further experiments. Furthermore, cotreatment with conjugates **6c**,

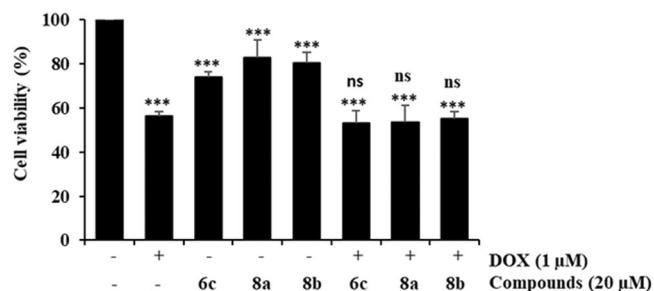


FIGURE 3 Bioactive conjugates **6c**, **8a**, and **8b** did not affect the antitumor effect of DOX in MCF-7 breast tumor cells. Cells were treated with compounds (20 μM) alone or in combination with DOX (1 μM) for 24 h. Cell viability was measured by MTT assay. Results are reported as the mean of cell viability \pm SD ($n = 3$). *** $p < .001$ versus untreated cells, ns = no significant versus DOX-treated cells. DOX, doxorubicin; LDH, lactate dehydrogenase; MTT, 3-(4,5-dimethylthiazol-2-yl)-2,5-diphenyl-2H-tetrazolium bromide; ns, not significant.

8a, and **8b** in the DOX cardiotoxicity model induced a significant decrease in LDH release, a marker of cellular damage (Figure 2d). The results obtained confirmed the protective effects of these three compounds, which were selected for further testing.

An important issue for the design of new cardioprotective compounds is that the reduction of DOX unwanted side effects should not compromise its antitumor potential. To further investigate whether labdane conjugates preserved the antitumor effect of DOX, MCF-7 breast cancer cells were treated with compounds alone or in combination with DOX. Results shown in Figure 3 demonstrated that the three tested diterpene conjugates **6c**, **8a**, and **8b** did not interfere with the DOX anticancer activities in MCF-7 cells.

From the obtained results, some structure–activity relationships were outlined. Among the labdane conjugates with a triazol linker (**6a**–**6c**), compound **6c** having a naphthalimide moiety was the only one that showed cardioprotective activity. Regarding the labdane–furonaphthoquinone conjugates (**8a**–**8d**), the nature of the moiety attached to the nitrogen seems to play an important role in the activity, since **8a** with a cyclohexyl substituent and **8b** with an ethylmorpholine group showed cardioprotective effects, while conjugates with a benzyl group (**8c**) or a *tert*-butyl (**8d**) resulted less active. These data suggest that this part of the molecule could interact with specific residues of the target and the resultant interactions cause the corresponding modulation of the activity.

Further investigations were focused on the molecular mechanisms of the cardioprotective properties of the selected compounds. Accumulation of ROS and autophagy dysfunction are considered important events in cardiotoxicity by DOX (Koleini & Kardami, 2017;

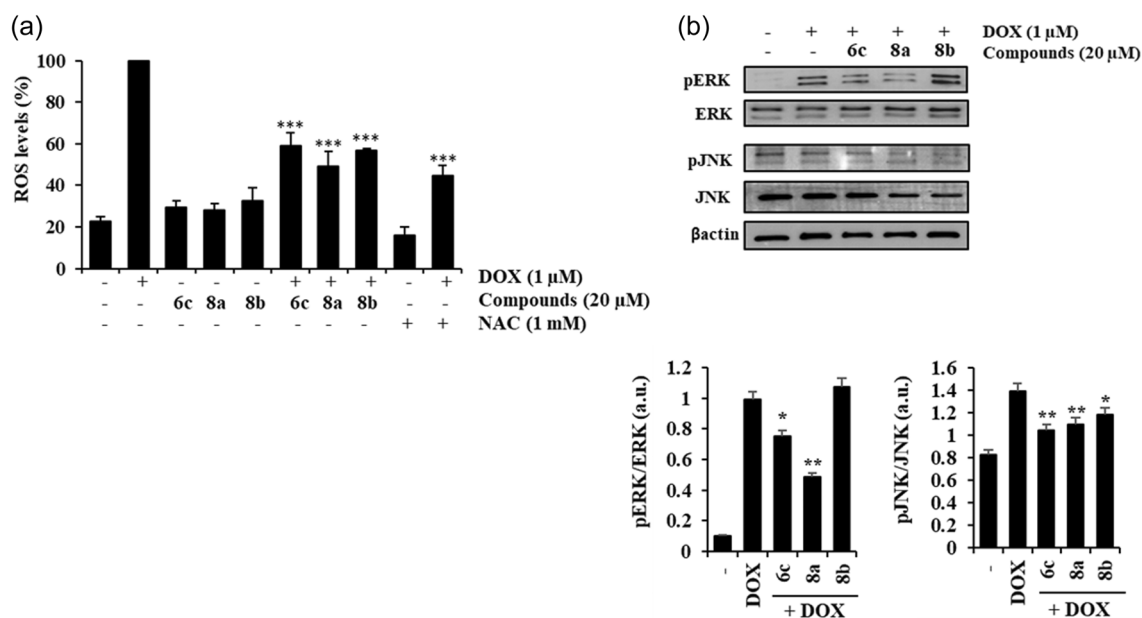


FIGURE 4 Labdane conjugates **6c**, **8a**, and **8b** diminished DOX-induced oxidative stress in cardiomyocytes. (a) Levels of ROS generation in H9c2 cells were measured fluorometrically after treatment with 1 μM DOX alone or cotreatment with *N*-acetyl cysteine (NAC, 1 mM) or conjugates (20 μM) for 24 h, using the 2',7'-dichlorofluorescein-diacetate (DCFH-DA) assay. (b) Western blot analysis of ERK and JNK expression in cells following exposure to DOX (1 μM) alone or in combination with conjugates (20 μM). β -Actin was immunoblotted as a loading control. Densitometric analysis of relative expression of pERK and pJNK. Data are presented as mean \pm SD ($n = 3$). DOX, doxorubicin; ERK, extracellular signal-regulated kinase; JNK, c-Jun N-terminal kinase. * $p < .05$, ** $p < .01$, and *** $p < .001$ versus DOX-treated cells.

Rawat et al., 2021; Songbo et al., 2019). Figure 4a showed that ROS generation induced by DOX was significantly reduced by cotreatment with the active conjugates **6c**, **8a**, and **8b** ($59.03 \pm 6.42\%$, $49.34 \pm 6.89\%$, and $56.78 \pm 1.98\%$, respectively) at $20 \mu\text{M}$. Evaluation of ROS-mediated MAPK signaling pathways (ERK and JNK) indicated that selected compounds, in particular **8a**, could not only inhibit DOX-induced ROS generation but also suppressed ERK and JNK activation induced by DOX (Figure 4b).

Various signaling pathways involved in autophagy regulation, including Akt/AMPK/m-TOR signaling, have been described to be critical mediators of DOX-induced cardiotoxicity (Chen et al., 2011; Dirks-Naylor, 2013; Timm & Tyler, 2020). The addition of selected

compounds, in particular, conjugate **8a**, protected cardiomyocytes, as deduced by the increase in Akt phosphorylation and impaired activation of AMPK. Moreover, treatment with conjugates reversed the increased expression of the autophagy marker p62 induced by DOX (Figure 5). These results indicate that autophagy could be potentially restored with the compounds.

To deepen the structural determinants responsible for the cardioprotective effect two new derivatives, furonaphthoquinones **9** and **10** were prepared as simplified fragments of the active labdane-furonaphthoquinone conjugate **8a** (Figure 6).

The effects of these derivatives on H9c2 cell viability were tested (Figure 7). The results obtained showed that compounds **9** and **10** did

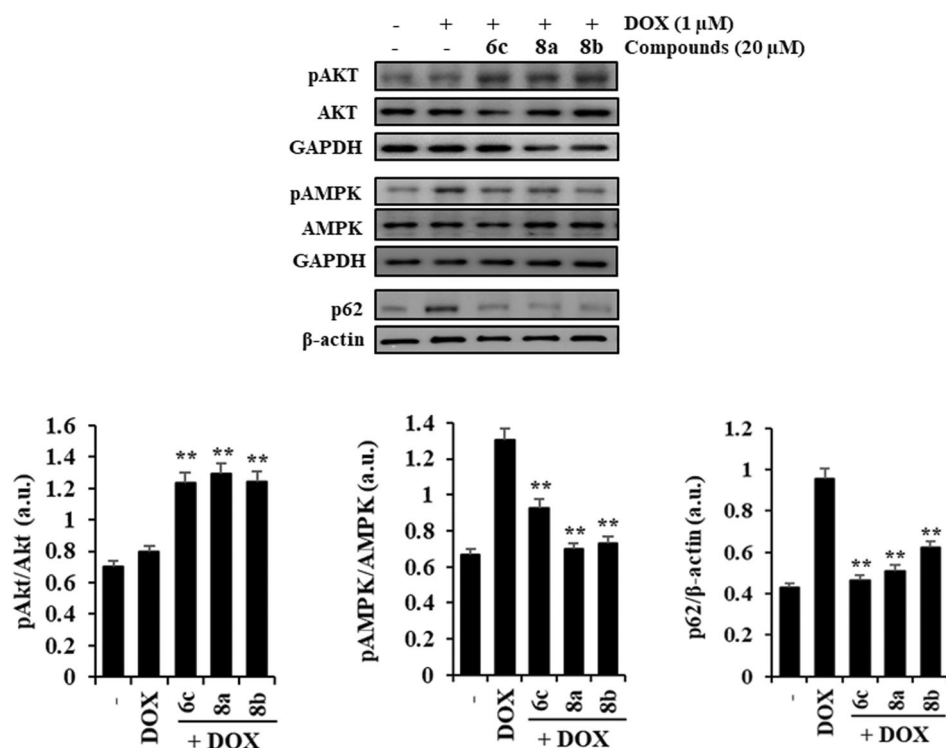


FIGURE 5 Bioactive conjugates **6c**, **8a**, and **8b** regulated DOX-induced activation of autophagy through Akt/AMPK. Immunoblot analysis of Akt, AMPK, and p62 in H9c2 cells following exposure to DOX ($1 \mu\text{M}$) alone or in combination with conjugates ($20 \mu\text{M}$). β -Actin and GAPDH were used as a loading control. A representative experiment of three performed is shown. DOX, doxorubicin, GAPDH, glyceraldehyde 3-phosphate dehydrogenase. ** $p < .01$ versus DOX-treated cells.

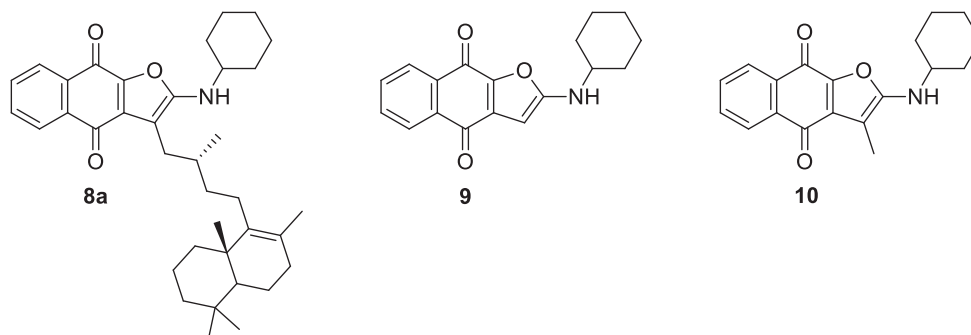


FIGURE 6 Structures of compounds **9** and **10** as simplified fragments of conjugate **8a**

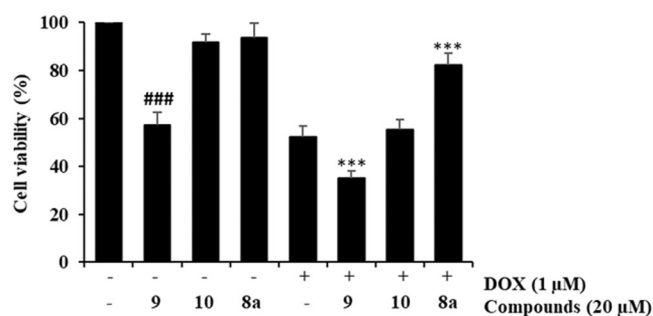


FIGURE 7 Evaluation of simplified derivatives **9** and **10**, and conjugate **8a** on DOX-induced cardiotoxicity. H9c2 cell viability was measured by MTT after incubation for 24 h with compounds (20 μM) in the absence or presence of DOX (1 μM). Results are reported as the mean of cell viability ± SD ($n = 3$). DOX, doxorubicin; MTT, 3-(4,5-dimethylthiazol-2-yl)-2,5-diphenyl-2H-tetrazolium bromide ^{###} $p < .001$ versus untreated cells and ^{***} $p < .001$ versus DOX-treated cells.

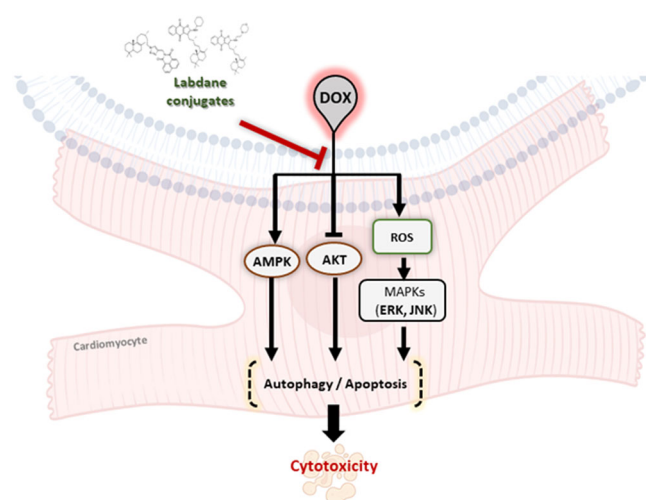


FIGURE 8 Schematic representation for the underlying mechanisms of cardioprotection by active labdane conjugates against DOX-induced toxicity. DOX, doxorubicin; ERK, extracellular signal-regulated kinase; JNK, c-Jun N-terminal kinase; ROS, reactive oxygen species. Created with [BioRender.com](https://www.biorender.com).

not exert any cardioprotective effects against DOX-induced toxicity in H9c2 cells. This indicates that the presence of both the diterpene unit and the furanophthoquinone moiety is relevant for cardioprotective effects, as the highest protection is achieved with compound **8a**. Targeted molecular pathways involved in the cardioprotective effects of active conjugates are summarized in Figure 8.

4 | CONCLUSIONS

To develop novel and effective cardioprotective agents, a series of labdane conjugates (**6a–6c** and **8a–8d**) were synthesized from the diterpene labdanodiol (**1**) and evaluated in an H9c2 cardiomyocyte model. Three labdane conjugates (**6c**, **8a**, and **8b**) displayed promising

results, improving the cell viability of DOX-treated myocardial cells. Molecular mechanisms involved in the protective effects were investigated. Active compounds exhibited a significant inhibition of oxidative stress and MAPK signaling. Among them, the labdane–furonaphthoquinone conjugate **8a** showed the best potential for cardioprotection via its additional ability to regulate upstream Akt/AMPK/mTOR signaling autophagic pathway in cardiomyocytes. To the best of our knowledge, this is the first ever report to show the cardioprotective potential of labdane diterpenes, in particular conjugates containing the furonaphthoquinone moiety, against DOX-induced cardiotoxicity. Thus, combined administration of labdane conjugates with DOX could improve the use of this chemotherapeutic agent, providing a safer strategy for cardioprotection.

ACKNOWLEDGMENTS

This study was supported by Grant RTI2018-094356-BC21 from the Ministerio de Ciencia, Innovación y Universidades (MICIU) to A. E.-B., I. C., L. G.-C., and B. H.; Grant PI17/00012 and PI20/00018 from the Instituto de Salud Carlos III to S. H. These projects are also cofunded by the European Regional Development Fund (FEDER). A. A. and S. O.-R. thank the Cabildo de Tenerife (Agustín de Betancourt Program).

CONFLICT OF INTEREST

The authors declare no conflict of interest.

DATA AVAILABILITY STATEMENT

The author has provided the required data availability statement, and if applicable, included functional and accurate links to said data therein.

ORCID

Sonsoles Hortelano <http://orcid.org/0000-0003-2528-0072>

Ana Estévez-Braun <http://orcid.org/0000-0001-5279-7099>

Beatriz de las Heras <http://orcid.org/0000-0001-5089-8988>

REFERENCES

- Abdullah, N. A., Md Hashim, N. F., Ammar, A., & Muhamad Zakuan, N. (2021). An insight into the anti-angiogenic and anti-metastatic effects of oridonin: Current knowledge and future potential. *Molecules*, 26(4), 775. <https://doi.org/10.3390/molecules26040775>
- Al-Malky, H. S., Al Harthi, S. E., & Osman, A. M. M. (2020). Major obstacles to doxorubicin therapy: Cardiotoxicity and drug resistance. *Journal of Oncology Pharmacy Practice*, 26(2), 434–444. <https://doi.org/10.1177/1078155219877931>
- Alzahrani, A. M., Rajendran, P., Veeraghavan, V. P., & Hanieh, H. (2021). Cardiac protective effect of kirenol against doxorubicin-induced cardiac hypertrophy in H9c2 cells through Nrf2 signaling via PI3K/AKT pathways. *International Journal of Molecular Sciences*, 22(6), 3269. <https://doi.org/10.3390/ijms22063269>
- Amaro-Luis, J. M., & Adrian, R. M. (1982). Diterpenoids of *Oxylobus glanduliferus* (Sch-Bip) Gray. *Revista Latinoamericana de Química*, 13, 110–113.
- Chen, M. B., Wu, X. Y., Gu, J. H., Guo, Q. T., Shen, W. X., & Lu, P. H. (2011). Activation of AMP-activated protein kinase contributes to doxorubicin-induced cell death and apoptosis in cultured myocardial H9c2 cells. *Cell Biochemistry and Biophysics*, 60(3), 311–322. <https://doi.org/10.1007/s12013-011-9153-0>

- Cuadrado, I., Cidre, F., Herranz, S., Estevez-Braun, A., de las Heras, B., & Hortelano, S. (2012). Labdanolic acid methyl ester (LAME) exerts anti-inflammatory effects through inhibition of TAK-1 activation. *Toxicology and Applied Pharmacology*, 258(1), 109–117. <https://doi.org/10.1016/j.taap.2011.10.013>
- Cuadrado, I., Fernández-Velasco, M., Boscá, L., & de las Heras, B. (2011). Labdane diterpenes protect against anoxia/reperfusion injury in cardiomyocytes: Involvement of AKT activation. *Cell Death & Disease*, 2, e229. <https://doi.org/10.1038/cddis.2011.113>
- Cuadrado-Berrolcal, I., Gómez-Gaviro, M. V., Benito, Y., Barrio, A., Bermejo, J., Fernández-Santos, M. E., Sánchez, P. L., Desco, M., Fernández-Avilés, F., Fernández-Velasco, M., Boscá, L., & de las Heras, B. (2015). A labdane diterpene exerts ex vivo and in vivo cardioprotection against post-ischemic injury: Involvement of AKT-dependent mechanisms. *Biochemical Pharmacology*, 93(4), 428–439. <https://doi.org/10.1016/j.bcp.2014.12.011>
- Dirks-Naylor, A. J. (2013). The role of autophagy in doxorubicin-induced cardiotoxicity. *Life Sciences*, 93(24), 913–916. <https://doi.org/10.1016/j.lfs.2013.10.013>
- Gao, R. F., Li, X., Xiang, H. Y., Yang, H., Lv, C. Y., Sun, X. L., Chen, H. Z., Gao, Y., Yang, J. S., Luo, W., Yang, Y. Q., & Tang, Y. H. (2021). The covalent NLRP3-inflammasome inhibitor oridonin relieves myocardial infarction induced myocardial fibrosis and cardiac remodeling in mice. *International Immunopharmacology*, 90, 107133. <https://doi.org/10.1016/j.intimp.2020.107133>
- Gong, H. H., Addla, D., Lv, J. S., & Zhou, C. H. (2016). Heterocyclic naphthalimides as new skeleton structure of compounds with increasingly expanding relational medicinal applications. *Current Topics in Medicinal Chemistry*, 16(28), 3303–3364. <https://doi.org/10.2174/1568026616666160506145943>
- Gong, P., Zhang, W., Zou, C., Han, S., Tian, Q., Wang, J., He, P., Guo, Y., & Li, M. (2022). Andrographolide attenuates blood-brain barrier disruption, neuronal apoptosis, and oxidative stress through activation of Nrf2/HO-1 signaling pathway in subarachnoid hemorrhage. *Neurotoxicity Research*, 40(2), 508–519. <https://doi.org/10.1007/s12640-022-00486-7>
- González-Cofrade, L., Oramas-Royo, S., Cuadrado, I., Amesty, Á., Hortelano, S., Estevez-Braun, A., & de las Heras, B. (2020). Dehydrohispanolone derivatives attenuate the inflammatory response through the modulation of inflammasome activation. *Journal of Natural Products*, 83(7), 2155–2164. <https://doi.org/10.1021/acs.jnatprod.0c00200>
- de las Heras, B., & Hortelano, S. (2009). Molecular basis of the anti-inflammatory effects of terpenoids. *Inflammation & Allergy Drug Targets*, 8(1), 28–39. <https://doi.org/10.2174/187152809787582534>
- Islam, M. T. (2017). Diterpenes and their derivatives as potential anticancer agents. *Phytotherapy Research*, 31(5), 691–712. <https://doi.org/10.1002/ptr.5800>
- Jiménez-Alonso, S., Guasch, J., Estévez-Braun, A., Ratera, I., Veciana, J., & Ravelo, A. G. (2011). Electronic and cytotoxic properties of 2-aminonaphtho[2,3-*b*]furan-4,9-diones. *The Journal of Organic Chemistry*, 76(6), 1634–1643. <https://doi.org/10.1021/jo102233j>
- Kamal, A., Bolla, N. R., Srikanth, P. S., & Srivastava, A. K. (2013). Naphthalimide derivatives with therapeutic characteristics: A patent review. *Expert Opinion on Therapeutic Patents*, 23(3), 299–317. <https://doi.org/10.1517/13543776.2013.746313>
- Koleini, N., & Kardami, E. (2017). Autophagy and mitophagy in the context of doxorubicin-induced cardiotoxicity. *Oncotarget*, 8(28), 46663–46680. <https://doi.org/10.18632/oncotarget.16944>
- Liang, D., Sun, Y., Shen, Y., Li, F., Song, X., Zhou, E., Zhao, F., Liu, Z., Fu, Y., Guo, M., Zhang, N., Yang, Z., & Cao, Y. (2013). Shikonin exerts anti-inflammatory effects in a murine model of lipopolysaccharide-induced acute lung injury by inhibiting the nuclear factor-kappaB signaling pathway. *International Immunopharmacology*, 16(4), 475–480. <https://doi.org/10.1016/j.intimp.2013.04.020>
- Luo, P., Wong, Y. F., Ge, L., Zhang, Z. F., Liu, Y., Liu, L., & Zhou, H. (2010). Anti-inflammatory and analgesic effect of plumbagin through inhibition of nuclear factor- κ B activation. *Journal of Pharmacology and Experimental Therapeutics*, 335(3), 735–742. <https://doi.org/10.1124/jpet.110.170852>
- Marco, J. L. (2020). Isolation, reactivity, pharmacological activities and total synthesis of hispanolone and structurally related diterpenes from Labiatae plants. *Bioorganic & Medicinal Chemistry Letters*, 30(21), 127498. <https://doi.org/10.1016/j.bmcl.2020.127498>
- Moon, D. O., Choi, Y. H., Kim, N. D., Park, Y. M., & Kim, G. Y. (2007). Anti-inflammatory effects of β -lapachone in lipopolysaccharide-stimulated BV2 microglia. *International Immunopharmacology*, 7(4), 506–514. <https://doi.org/10.1016/j.intimp.2006.12.006>
- Octavia, Y., Tocchetti, C. G., Gabrielson, K. L., Janssens, S., Crijns, H. J., & Moens, A. L. (2012). Doxorubicin-induced cardiomyopathy: From molecular mechanisms to therapeutic strategies. *Journal of Molecular and Cellular Cardiology*, 52(6), 1213–1225. <https://doi.org/10.1016/j.jymcc.2012.03.006>
- Perrin, D. D., & Amarego, W. L. F. (1988). *Purification of laboratory chemicals* (3rd ed.). Pergamon Press.
- Prathumsap, N., Shinlapawittayatorn, K., Chattipakorn, S. C., & Chattipakorn, N. (2020). Effects of doxorubicin on the heart: From molecular mechanisms to intervention strategies. *European Journal of Pharmacology*, 866, 172818. <https://doi.org/10.1016/j.ejphar.2019.172818>
- Rawat, P. S., Jaiswal, A., Khurana, A., Bhatti, J. S., & Navik, U. (2021). Doxorubicin-induced cardiotoxicity: An update on the molecular mechanism and novel therapeutic strategies for effective management. *Biomedicine & Pharmacotherapy*, 139, 111708. <https://doi.org/10.1016/j.biopha.2021.111708>
- Rostovtsev, V. V., Green, L. G., Fokin, V. V., & Sharpless, K. B. (2002). A stepwise Huisgen cycloaddition process: Copper(I)-catalyzed regioselective “ligation” of azides and terminal alkynes. *Angewandte Chemie International Edition*, 41(14), 2596–2599. [https://doi.org/10.1002/1521-3773\(20020715\)41:14<2596::AID-ANIE2596>3.0.CO;2-4](https://doi.org/10.1002/1521-3773(20020715)41:14<2596::AID-ANIE2596>3.0.CO;2-4)
- Soares, A. S., Barbosa, F. L., Rüdiger, A. L., Hughes, D. L., Salvador, M. J., Zampronio, A. R., & Stefanello, M. É. A. (2017). Naphthoquinones of *Sinningia reitzii* and anti-inflammatory/antinociceptive activities of 8-Hydroxydehydrodunnione. *Journal of Natural Products*, 80(6), 1837–1843. <https://doi.org/10.1021/acs.jnatprod.6b01186>
- Song, Z., Wang, L., Cao, Y., Liu, Z., Zhang, M., Zhang, Z., Jiang, S., Fan, R., Hao, T., Yang, R., Wang, B., Guan, Z., Zhu, L., Liu, Z., Zhang, S., Zhao, L., Xu, Z., Xu, H., & Dai, G. (2022). Isoandrographolide inhibits NLRP3 inflammasome activation and attenuates silicosis in mice. *International Immunopharmacology*, 105, 108539. <https://doi.org/10.1016/j.intimp.2022.108539>
- Songbo, M., Lang, H., Xinyong, C., Bin, X., Ping, Z., & Liang, S. (2019). Oxidative stress injury in doxorubicin-induced cardiotoxicity. *Toxicology Letters*, 307, 41–48. <https://doi.org/10.1016/j.toxlet.2019.02.013>
- Tanaka, S., Tajima, M., Tsukada, M., & Tabata, M. (1986). A comparative study on anti-inflammatory activities of the enantiomers, shikonin and alkannin. *Journal of Natural Products*, 49(3), 466–469. <https://doi.org/10.1021/np50045a014>
- Timm, K. N., & Tyler, D. J. (2020). The role of AMPK activation for cardioprotection in doxorubicin-induced cardiotoxicity. *Cardiovascular Drugs and Therapy*, 34(2), 255–269. <https://doi.org/10.1007/s10557-020-06941-x>
- Tran, Q. T. N., Wong, W. S. F., & Chai, C. L. L. (2017). Labdane diterpenoids as potential anti-inflammatory agents. *Pharmacological Research*, 124, 43–63. <https://doi.org/10.1016/j.phrs.2017.07.019>
- Través, P. G., López-Fontal, R., Cuadrado, I., Luque, A., Boscá, L., de las Heras, B., & Hortelano, S. (2013). Critical role of the death receptor pathway in the antitumoral effects induced by hispanolone

- derivatives. *Oncogene*, 32(2), 259–268. <https://doi.org/10.1038/onc.2012.23>
- Tseng, C. H., Cheng, C. M., Tzeng, C. C., Peng, S. I., Yang, C. L., & Chen, Y. L. (2013). Synthesis and anti-inflammatory evaluations of β -lapachone derivatives. *Bioorganic & Medicinal Chemistry*, 21(2), 523–531. <https://doi.org/10.1016/j.bmc.2012.10.047>
- Wang, T., Wu, F., Jin, Z., Zhai, Z., Wang, Y., Tu, B., Yan, W., & Tang, T. (2014). Plumbagin inhibits LPS-induced inflammation through the inactivation of the nuclear factor-kappa B and mitogen-activated protein kinase signaling pathways in RAW 264.7 cells. *Food and Chemical Toxicology*, 64, 177–183. <https://doi.org/10.1016/j.fct.2013.11.027>
- Yang, Y., Yang, W. S., Yu, T., Yi, Y. S., Park, J. G., Jeong, D., Kim, J. H., Oh, J. S., Yoon, K., Kim, J. H., & Cho, J. Y. (2014). Novel anti-inflammatory function of NSC95397 by the suppression of multiple kinases. *Biochemical Pharmacology*, 88(2), 201–215. <https://doi.org/10.1016/j.bcp.2014.01.022>
- Yu, J., Wang, C., Kong, Q., Wu, X., Lu, J. J., & Chen, X. (2018). Recent progress in doxorubicin-induced cardiotoxicity and protective

potential of natural products. *Phytomedicine*, 40, 125–139. <https://doi.org/10.1016/j.phymed.2018.01.009>

SUPPORTING INFORMATION

Additional supporting information can be found online in the Supporting Information section at the end of this article.

How to cite this article: Cuadrado, I., Oramas-Royo, S., González-Cofrade, L., Amesty, Á., Hortelano, S., Estévez-Braun, A., & las Heras, B. d (2023). Labdane conjugates protect cardiomyocytes from doxorubicin-induced cardiotoxicity. *Drug Development Research*, 84, 84–95. <https://doi.org/10.1002/ddr.22014>